



Mechanistic role of each metal ion in *Streptomyces* dinuclear aminopeptidase: Peptide hydrolysis and 7×10^{10} -fold rate enhancement of phosphodiester hydrolysis

Altan Ercan¹, William M. Tay, Steven H. Grossman, Li-June Ming*

Department of Chemistry and Institute for Biomolecular Science, University of South Florida, 4202 E. Fowler Avenue, CHE205, Tampa, FL 33620-5250, USA

ARTICLE INFO

Article history:

Received 10 March 2009
Received in revised form 22 September 2009
Accepted 23 September 2009
Available online 29 September 2009

Keywords:

Aminopeptidase
Catalytic promiscuity
Dinuclear
Manganese
NMR
Streptomyces

ABSTRACT

The dinuclear aminopeptidase from *Streptomyces griseus* (SgAP) and its metal derivatives catalyze the hydrolysis of the phosphoester bis(*p*-nitrophenyl) phosphate (BNPP) and the phosphonate ester *p*-nitrophenyl phenylphosphonate with extraordinary rate enhancements at pH 7.0 and 25 °C [A. Ercan, H. I. Park, L.-J. Ming, *Biochemistry* 45, (2006) 13779–13793.], reaching 6.7 billion-fold in terms of the first-order rate constant of the di-Co(II) derivative with respect to the autohydrolytic rates. Since phosphoesters are transition state-like inhibitors in peptide hydrolysis, their hydrolysis by SgAP is quite novel. Herein, we report the investigation of this proficient alternative catalysis of SgAP and the role of each metal ion in the dinuclear site toward peptide and BNPP hydrolysis. Mn(II) selectively binds to one of the dinuclear metal sites (M1), affording MnE-SgAP with an empty (*E*) second site for the binding of another metal (M2), including Mn(II), Co(II), Ni(II), Zn(II), and Cd(II). Peptide hydrolysis is controlled by M2, wherein the k_{cat} values for the derivatives MnM2-SgAP are different yet similar between MnCo- and CoCo-SgAP and pairs of other metal derivatives. On the other hand, BNPP hydrolysis is affected by metals in both sites. Thus, the two hydrolytic catalyses must follow different mechanisms. Based on crystal structures, docking, and the results presented herein, the M1 site is close to the hydrophobic specific site and the M2 site is next to Tyr246 that is H-bonded to a coordinated nucleophilic water molecule in peptide hydrolysis; whereas a coordinated water molecule on M1 becomes available as the nucleophile in phosphodiester hydrolysis.

© 2009 Elsevier Inc. All rights reserved.

1. Introduction

Enzymes can effect remarkable rate accelerations by stabilizing the transition-state (TS[‡]) of the substrates [1]. The use of TS[‡] analogues for the production of catalytic antibodies [2] and inhibition of peptidases and esterases by different phospho-centers [3–6] support the TS[‡] theory. However, some phosphoesters and fluoro-phosphates can be hydrolyzed by serine proteases and esterases via nucleophilic attack by the active-site Ser [7], which nevertheless produces an indefinitely stable dead-end complex with the phospho-center covalently attached to the Ser. Moreover, the phosphoester bis(*p*-nitrophenyl)phosphate (BNPP) and the phosphonate ester *p*-nitrophenyl phenylphosphonate can be effectively hydrolyzed by the dinuclear aminopeptidase (AP) from *Streptomyces griseus* (SgAP) with activities comparable to some native phospho-

hoesterases [8–10]. Since phospho- and phosphono-esters are TS[‡]-like molecules and can inhibit peptide hydrolysis [11–13], their hydrolysis by SgAP is novel and must take place according to a unique catalytic pathway of the enzyme.

SgAP (30 kDa) is a Ca²⁺-influenced extracellular enzyme of high thermal stability with a catalytic specificity toward hydrophobic substrates [14,15]. It has a di-metal center (3.65 Å apart) bound to the protein through the side chains of His85 and Asp160 in one metal site and His247 and Glu132 in another site, along with a bridging Asp97 [16,17]. SgAP and the AP from *Aeromonas proteolytica* (ApAP, 32 kDa) have 29.6% sequence identity, identical metal-binding ligands, and a similar three-dimensional structure [18]. However, ApAP [19] along with mammalian AP-P and *Escherichia coli* Met AP [20–22] require only one metal to activate, and a second metal to modulate, its activity. Conversely, SgAP requires two metal ions for catalysis on the basis of crystallographic, NMR, and kinetic studies [8–10,19,23–25].

The active site of metalloenzymes can be investigated with spectroscopic and kinetic methods by the use of various metal ions [26–29]. Different homo- and hetero-dinuclear derivatives of dinuclear APs, including Leu-specific APs from bovine lens (bILAP) [29]

* Corresponding author. Tel.: +1 813 974 2220; fax: +1 813 974 3203.

E-mail address: ming@shell.cas.usf.edu (L.-J. Ming).

¹ Present address: Division of Rheumatology, Immunology and Allergy, Brigham and Women's Hospital, Harvard Medical School, Smith Building, Room 536, 1 Jimmy Fund Way, Boston, MA 02115, USA.

and porcine kidney (pkLAP) [30] and ApAP [19], were constructed and investigated to gain further insight into the function of each metal ion in catalysis [19,31]. For example, in bLAP, the first metal-binding site shows higher effect on k_{cat} while the second metal is more influential on K_{m} [29]. On the other hand, the first Zn^{2+} affects K_{m} while the second metal affects k_{cat} in pkLAP [30] and both k_{cat} and K_{m} values are affected by the two metals in ApAP [32]. The variations of the kinetic parameters with the different metal derivatives of these enzymes signifies the importance and the function of each metal ion in their dinuclear active center.

Different metal derivatives of ApAP were prepared and their activity and inhibition by 1-butaneboronic acid investigated, from which a mononuclear mechanism was proposed [33–35]. The crystal structure of ZnZn-ApAP upon binding with this inhibitor shows that the inhibitor binds one metal through two oxygen atoms, one of which may interact with the second metal [36]. Unlike ApAP, SgAP is inactive with only one metal and becomes fully active upon binding of the second metal [23]. In this case, selective Co^{2+} binding has been verified with NMR, showing distinct hyperfine-shifted ^1H NMR signals for Co,E- and Co,Co-SgAP [23]. Since selective metal-binding of SgAP occurs, different metal ions can be introduced to construct various hetero-dinuclear derivatives. We present herein further investigation of the role of each metal ion in the dinuclear active site in the action of SgAP by the use of various hetero-dinuclear derivatives MnM2-SgAP (M2 = Zn^{2+} , Co^{2+} , Ni^{2+} , or Cd^{2+}). The mechanisms of this enzyme toward the hydrolysis of peptides and the alternative hydrolysis of BNPP are proposed.

2. Experimental section

2.1. Materials and reagents

The protease mixture Pronase, the buffers, HEPES, MES, NaH_2PO_4 , EDTA, 1,10-phenanthroline, phenylglyoxal monohydrate, DEAE-Sephacel and Sephadex G-50, the substrate L-Leu-p-nitroanilide (Leu-pNA), Met-pNA, Val-pNA, Ala-pNA, Gly-pNA, and BNPP were purchased from Sigma-Aldrich (St. Louis, MO) and the atomic absorption standards (>99.99%) of Zn^{2+} , Co^{2+} , Mn^{2+} , Cd^{2+} , Ni^{2+} , and Cu^{2+} from Fisher Scientific (Pittsburg, PA). Deionized water of >18 M Ω obtained from a MilliQ system (Millipore, Bedford, MA) was used to prepare all the solutions. All the glassware and plastic ware were treated with 2 mM EDTA solution and rinsed with deionized water prior to use.

2.2. Purification, demetallization, and characterization of SgAP

SgAP was purified according to the published procedures [14,23]. The fractions of the first peak from the DEAE-Sephacel column with AP activity were combined. Purified SgAP (0.05–0.1 mM, 10 ml) was dialyzed for 12 h against 250 ml of 20 mM Tris/HCl buffer at pH 7.5 with 100 mM NaCl for four times, with 2.0 mM EDTA and 2.0 mM 1,10-phenanthroline for the first two times and 2.0 mM 1,10-phenanthroline for latter two, followed by dialyzing against 250 ml of 20 mM MES at pH 6.0 for four times to remove the chelators. The AP concentration was determined according to the absorption $E_{280}^{1\%} = 15$ [14,23] and by titration with atomic-absorption-grade Co^{2+} solution of known concentrations.

The formation of the various MnM-SgAP derivatives was verified by their activities and after prolonged incubation to ensure the retention of the activities (otherwise, migration of metal ions in the two sites may take place). Paramagnetically shifted ^1H NMR features were also used as the fingerprints for identification of the Co^{2+} -containing derivatives [37–39]. The ^1H NMR spectra of the paramagnetic derivatives were acquired on a Varian INOVA500 spectrometer (at 500 MHz ^1H resonance) with a 5-mm

bio-TR (triple resonance) probe by the use of the build-in polynomial 1–3–3–1 pulse sequence for samples in H_2O buffers and a pre-saturation pulse for samples in D_2O buffers with a 90° pulse of $\sim 9 \mu\text{s}$ over 200 ppm spectral width and processed with a line-broadening of 40 Hz, followed by spline baseline correction.

2.3. Enzyme kinetics and inhibition

The kinetics was carried out in 0.1 M HEPES buffer at pH 8.0 containing 0.1 M NaCl and 10 mM CaCl_2 at 30°C and the data were analyzed with the Michaelis–Menten model to derive the turnover k_{cat} and the Michaelis constant K_{m} with non-linear fitting of the rate with respect to substrate concentration. Fluoride inhibition was carried out under the same conditions with different inhibitor concentrations, but in the absence of Ca^{2+} to avoid the formation of the very insoluble CaF_2 . Each inhibition study was performed at least twice and fitted to the Michaelis–Menten equation with non-linear regression and the inhibition constants K_i for different inhibition patterns are determined accordingly.

2.4. pH Profiles and thermostability

Catalytic parameters (k_{cat} and K_{m}) toward hydrolysis of Leu-pNA and BNPP and inhibitions were measured at different pHs (acetate at pH 5.0, MES at 5.5–6.5, HEPES at 7.0–8.0, TAPS at 8.5–9.5, and CAPS at 10.0). Thermostability of apo-SgAP and different metal derivatives of SgAP was determined on the basis of their activities toward Leu-pNA hydrolysis. Herein, SgAP and its various metal derivatives with or without 5 mM CaCl_2 were incubated at various temperatures for 1.0 min followed by incubation on ice for 5 min. Then, an excess amount of corresponding metal was added and activity determined.

3. Results and discussion

3.1. Mn^{2+} binding and hetero-dinuclear active site of SgAP

The binding of Mn^{2+} to apo-SgAP at pH 6.0 requires >50 equivalents to fully activate the enzyme (Fig. 1A), wherein the activity is significantly enhanced by Ca^{2+} (5 mM). At pH 8.0 without Ca^{2+} , Mn^{2+} binds to one site exclusively without showing activity (o, Fig. 1B and inset), and reaches full activation at >20 equivalents. Mn^{2+} binding becomes less selective and the enzyme is 44% less active in the presence of Ca^{2+} (●, Fig. 1B and inset). The binding of Mn^{2+} to just one metal-binding site in the active center at one equivalent (denoted the M1 site) allows the introduction of another metal ion to the second site (M2) to construct several catalytically active hetero-dinuclear derivatives in the form of Mn,M2-SgAP (where M2 = Co^{2+} , Zn^{2+} , Ni^{2+} , or Cd^{2+}) (Fig. 1C). Conversely, the binding of Zn^{2+} , Cd^{2+} , or Cu^{2+} to the enzyme exhibit a non-selective pattern [23,24,40], preventing the preparation of the corresponding M1,E-SgAP derivatives with an empty (E) M2 site. The first equivalent of Mn^{2+} must bind to the active site of SgAP. Otherwise, the subsequent addition of one equivalent of Co^{2+} (▼, Fig. 1C) would not generate an active derivative since CoE-SgAP is inactive [23].

The derivative MnCo-SgAP shows paramagnetically shifted ^1H NMR features in the downfield region ~ 30 – 80 ppm (Fig. 2, bottom) different from those of CoE- [23] and CoZn-SgAP [41], indicating a new Co^{2+} derivative. The spectrum is also different from that of CoCo-SgAP which indicates that Co^{2+} is not bound to both metal site of the protein (by replacing the Mn^{2+}). The NMR signals of the protons around mononuclear Mn^{2+} cannot be detected due to signal broadening by the slowly relaxing unpaired electrons of Mn^{2+} . However, magnetic coupling between Mn^{2+} and a metal

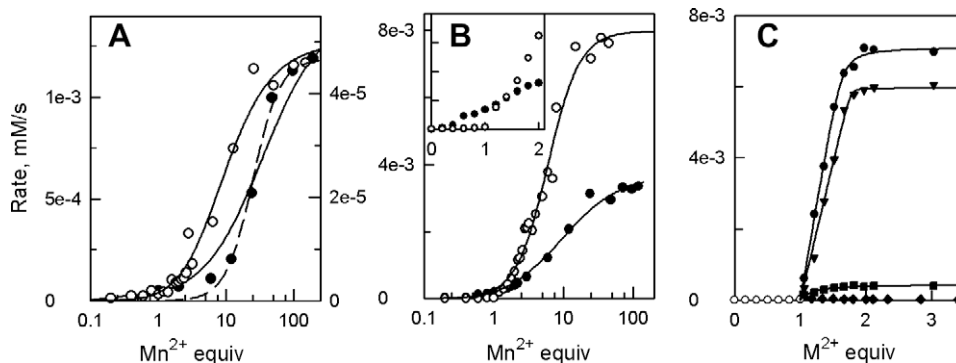


Fig. 1. (A) Mn^{2+} titration into apo-SgAP (20 μM) in the presence (●; left scale) and absence (○; right scale) of 5 mM CaCl_2 in 20 mM MES at pH 6.0. (B) Apo-SgAP (20 μM) is titrated with Mn^{2+} in the absence (○) and presence (●) of 5 mM Ca^{2+} in 20 mM HEPES at pH 8.0. The inset shows the binding of the first 2 equivalents of Mn^{2+} . (C) Apo-SgAP (20 μM) was titrated with Mn^{2+} (○) up to one equivalent followed by the addition of Zn^{2+} (●), Co^{2+} (▼), Cd^{2+} (■), or Ni^{2+} (◆) in 20 mM HEPES at pH 8.0. All the metal bindings are monitored with the activity toward the hydrolysis of 1.5 mM Leu-pNA in the absence of Ca^{2+} at 30 °C. The data in (A) and (B) were fitted to a sequential metal-binding model wherein the binding of the first equivalent (Mn1) results in an inactive derivative Mn1-SgAP, i.e., $\text{Mn1} + \text{SgAP} \rightleftharpoons \text{Mn1-SgAP}$ with a formation constant of $K_{f1} = [\text{Mn1-SgAP}]/[\text{Mn1}][\text{SgAP}]$, while the subsequent binding of the second equivalent (Mn2) forms the active Mn1Mn2-SgAP, i.e., $\text{Mn2} + \text{Mn1-SgAP} \rightleftharpoons \text{Mn1Mn2-SgAP}$ with a formation constant $K_{f2} = [\text{Mn1Mn2-SgAP}]/([\text{Mn2}][\text{Mn1-SgAP}])$ [24]. The dashed trace in (A) was fitted to the Hill's equation with a Hill's coefficient of -2.17 . The data in (C) were fitted to the equilibrium $\text{M2} + \text{Mn1-SgAP} \rightleftharpoons \text{Mn1M2-SgAP}$ ($K_{f2} = [\text{Mn1M2-SgAP}]/([\text{M2} + 1 \text{ equiv}][\text{Mn1-SgAP}])$) after the addition of 1 equivalent of Mn^{2+} to apo-SgAP.

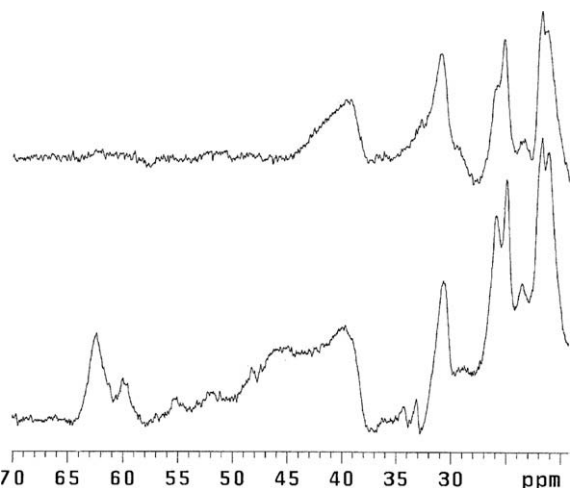


Fig. 2. ^1H NMR spectra (500 MHz) of 0.7 mM MnCo-SgAP in H_2O (bottom) and D_2O (top) (20 mM MES at pH 6.0).

ion of fast electron relaxation, such as high-spin Co^{2+} and Fe^{2+} , in a dinuclear center can afford hyperfine-shifted ^1H NMR signals due to both the Mn^{2+} and the other metal sites [37–39]. Thus, the observed hyperfine-shifted ^1H NMR signals herein can only result from the dinuclear MnCo-SgAP. Two solvent exchangeable signals are detected at 59.8 and 62.5 ppm which disappear in the sample prepared in a D_2O buffer (Fig. 2, top). These signals are consistent with the imidazole NH proton of coordinated His residues, one in each metal site (His85 and His247) [16,17]. The broad signals at ~ 45 ppm seems to be solvent exchangeable; however, the broadness of this signal prevents its assignment at this stage.

In order to use these hetero-dinuclear derivatives for kinetic studies, it is essential to prove that the two metal ions do not switch their binding positions with each other during the time span of the experiment. If metal ions in M1, M2-SgAP would switch their positions, different k_{cat} and K_m values would be expected. To verify this, the kinetic parameters were determined immediately after MnCo-SgAP was prepared and a day later, which showed no difference. Moreover, ^1H NMR does not reveal any hyperfine-shifted ^1H NMR signals characteristic of CoE-SgAP or CoCo-SgAP within a week which also supports the conclusion that there is no metal exchange between the two sites in MnCo-SgAP.

A few equivalents of Cd^{2+} are required to saturate the active site of SgAP to exhibit full activity [24]. However, one equivalent of Cd^{2+} is able to activate MnE-SgAP (■, Fig. 1C), suggesting that binding of Mn^{2+} may organize the active site for better binding of the second metal ion to exhibit activity. Nevertheless, the Cd^{2+} affinity toward MnE-SgAP is still ~ 400 and ~ 6000 times weaker than Zn^{2+} and Co^{2+} affinity (Fig. 1C).

The various metal derivatives of SgAP presumably should exhibit thermostability to different extents, thus can be further characterized. Apo-SgAP in the absence of CaCl_2 is the least stable, showing 50% denaturation ($T_{50\%}$) at ~ 60 °C within 1.0 min determined from activity measurements (Fig. 3A). The influence of transition metal ions on the stability is quite pronounced, wherein the one-metal derivatives CoE- and MnE-SgAP show $T_{50\%}$ at ~ 68 °C; MnCo-SgAP, ~ 80 °C; and other dimetal derivatives, >85 °C. In the presence of 5.0 mM CaCl_2 , all forms of SgAP are dramatically stabilized. For example, apo-SgAP shows $T_{50\%}$ at ~ 83 °C while MnMn-SgAP is still fully active even at 85 °C for a minute. The results support the conclusion from metal-titration experiments that Mn^{2+} indeed binds to apo-SgAP to form the derivative MnE-SgAP which exhibits a thermo-denaturation pattern different from those of MnMn-SgAP and apo-SgAP without Ca^{2+} (Fig. 3A). If the lack of activity of the enzyme with <1.0 equivalent Mn^{2+} (Fig. 1C) is due

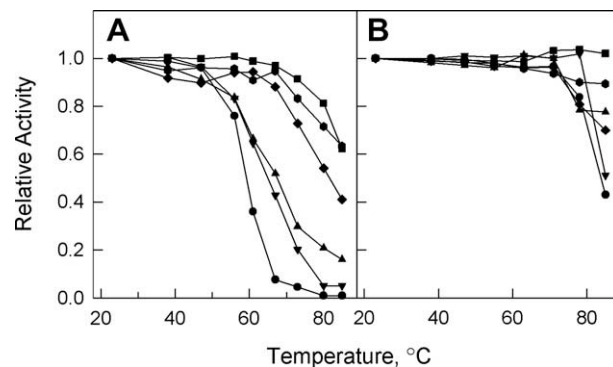


Fig. 3. Temperature-dependent denaturation of (A) apo-, MnE-, CoE-, MnCo-, CoCo-, and MnMn-SgAP (from bottom to top at 80 °C) and (B) Apo-, MnE-, MnCo-, CoE-, CoCo-, and MnMn-SgAP in the presence of 5-mM Ca^{2+} (from bottom to top at 85 °C) at 1.0 μM during the incubation and 0.01 μM in the assay toward the hydrolysis of 1.0 mM Leu-pNA at room temperature in 0.1 M HEPES at pH 8.0.

to that the metal is not bound to the enzyme, there should be little activity at $\sim 70^\circ\text{C}$ as that of apo-SgAP, which is not the case.

3.2. Fluoride inhibition

The inhibition by F^- toward Leu-pNA hydrolysis by MnMn-SgAP exhibits an uncompetitive inhibition pattern (Fig. 4A), indicating F^- binding to the ES complex. Uncompetitive F^- inhibition of metallo-enzymes has been suggested to be associated with the status of the nucleophilic water [25,42–47]. In the case of urease, purple acid phosphatase, and tyrosinase, F^- is proposed to replace the bridging hydroxide. The F^- inhibition toward Leu-pNA hydrolysis is uncompetitive at pH 7.5 to 10.0 with a gradual increase in K_i from 0.24 to 19.4 mM (Fig. 5C), showing an ionization constant $\text{p}K_a$ of 9.2 in the $\text{p}K_i$ -vs.-pH plot. A similar $\text{p}K_a$ is also observed in the pH profile of k_{cat}/K_m (discussed below). Because F^- replaces prospective nucleophile, the $\text{p}K_i$ -pH profile should reveal the ionization of the amino acid that influences the generation of the nucleophile, likely Tyr246 which has been implied to interact with a coordinated water [16]. Moreover, ApAP does not contain a corresponding Tyr and does not decrease in activity associated with a $\text{p}K_a$ in the alkaline range [48].

F^- also inhibits the various metal derivatives of SgAP in an uncompetitive manner, wherein the inhibition constant is significantly influenced by the metal ions in the active site (Table 1), more so by M2 as in the influence on the catalysis by M2. For example, the K_i values of MnMn-, MnNi-, and MnCo-SgAP are quite different, but closer for the counterparts M1,Ni- and M1,Co-SgAP (Table 1). Evidences from NMR, EPR, and resonance Raman studies of purple acid phosphatase (PAP) show that binding of F^- interrupts the metal-metal interaction, indicating that F^- interacts with both metal ions and the nucleophile in PAP (and urease as well) is proposed to be the bridging $\text{H}_2\text{O}/\text{OH}^-$ [44,45]. However, since only one metal (M2) is significantly associated with F^- inhibition in the case of SgAP, the nucleophile in this enzyme must be a terminal OH^- .

In a recent report, both F^- (0–80 mM) and phosphate (0–50 mM) were observed to exhibit noncompetitive inhibition toward native SgAP [49], different from what we observed previously [10] and described herein. The addition of CaCl_2 to the enzyme can activate the enzyme significantly [14], while phosphate or F^- therein can presumably remove the added 1 mM Ca^{2+} due to the very low K_{sp} of $\text{Ca}(\text{HPO}_4)/\text{Ca}_3(\text{PO}_4)_2$ and CaF_2 . The removal of Ca^{2+} would decrease the enzyme activity in a noncompetitive manner. Thus, the study cannot reveal clear inhibition patterns of phosphate and fluoride toward the enzyme itself and is not comparable to what we previously reported [10] and presented herein without the activator Ca^{2+} .

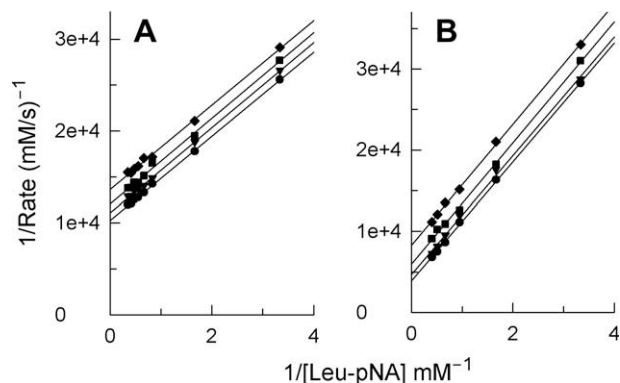


Fig. 4. Fluoride inhibition of (A) MnMn-SgAP (2.5 nM) at $[\text{F}^-] = 0.00, 75.0, 225,$ and $600 \mu\text{M}$ (from bottom) and (B) MnZn-SgAP (1.0 nM) at $[\text{F}^-] = 0.0, 20, 40,$ and 80 mM (from bottom) toward the hydrolysis of Leu-pNA in 20 mM HEPES at pH 8.0.

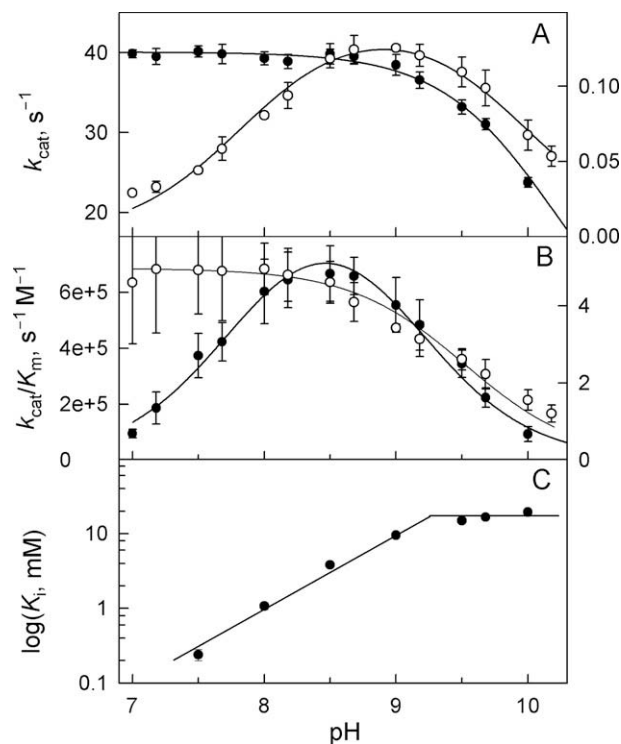


Fig. 5. Influence of pH on the activity of MnMn-SgAP toward Leu-pNA hydrolysis (2.5 nM; ●, left scales) and BNPP hydrolysis (0.20 μM ; ○, right scales) and on F^- inhibition (C) toward Leu-pNA hydrolysis. At pHs lower than 8.5, Mn^{2+} concentration was 100 μM while at the higher pHs, it was 50 μM to ensure full Mn^{2+} binding to the active site. The bell-shaped data set were fitted to $k = k_{\text{lim}}/((1 + [\text{H}^+]/K_{a1})(1 + K_{a2}/[\text{H}^+]))$ while the titration-like data set were fitted to $k = k_{\text{lim}}/(1 + K_{a2}/[\text{H}^+])$ with non-linear regression.

3.3. Activity-pH profile of MnMn-SgAP

The pH dependence of k_{cat} in Leu-pNA hydrolysis by MnMn-SgAP in the range of pH 7–10.5 is controlled by only one ionization constant $\text{p}K_{\text{es}} = 10.2$ (●, Fig. 5A, left scales; Table 2), likely attributed to Tyr246 since heat of ionization (28.5 kJ/mol) for this $\text{p}K_a$ in native SgAP is comparable to that of Tyr (~ 25 kJ/mol) [10]. The activities at lower pHs were not obtainable due to instability of the enzyme. The pH dependence of k_{cat}/K_m is controlled by two ionization constants $\text{p}K_e$ of 7.8 and 9.1 (●, Fig. 5B, left scales; Table 2), due to ionizations in the free enzyme and/or the free substrate. The $\text{p}K_a$ of 7.8 in the pH profile of k_{cat}/K_m for the hydrolysis of Leu-pNA by di-Mn-SgAP (and the $\text{p}K_a$ values of 7.6 and 7.4 in native di-Zn ApAP [48] and SgAP [10]) is much higher than that of a coordinated nucleophilic water in the mononuclear metallopeptidases carboxypeptidase A (6.3) [50], thermolysin (5.1) [51], and serralsin (5.74) [52]. This comparison suggests that this $\text{p}K_a$ may not be due to a coordinated water, but most likely the amino group of the substrate ($\text{p}K_a = 7.94$) [10] which is consistent with that deprotonation and binding of the amino group of the substrate controls the activity as suggested in the catalysis by bILAP [53]. Moreover, this $\text{p}K_a$ is much higher than those values of the few mononuclear metallopeptidases above, suggesting that it is not likely to be attributed to a bridging water since the latter is expected to be lower due to binding to two Lewis acidic metal centers.

The pH dependence of k_{cat} in BNPP hydrolysis shows two deprotonation constants $\text{p}K_{\text{es}}$ of 7.8 and 10.0 in the range of pH 7 to 10.5, while k_{cat}/K_m is controlled by only one $\text{p}K_{\text{e}2}$ of 9.5 (Fig. 5, ○, right scales; Table 2) which is comparable to one in Leu-pNA hydrolysis by MnMn- and ZnZn-SgAP [10]. A comparison of the pH profiles for the hydrolysis of Leu-pNA and BNPP indicates that the decrease in

Table 1

Kinetic parameters of homo- and hetero-dinuclear M1M2-SgAP toward the hydrolysis of Leu-pNA in 20 mM HEPES at pH 8.0.

M ₁ M ₂ -SgAP	k_{cat} (s ⁻¹)	CP ^a ($\times 10^6$)	K_m (mM)	k_{cat}/K_m (mM ⁻¹ s ⁻¹)	K_i (mM) ^b
ZnZn [10]	101 ± 3	6700	3.27 ± 0.17	30.9	108 ± 24
MnZn	92.8 ± 1.1	950	3.31 ± 0.06	28.0	70 ± 19
CdCd	1.68 ± 0.05	17	0.213 ± 0.020	7.89	–
MnCd	1.50 ± 0.04	15	0.190 ± 0.020	7.89	–
CoCo	41.0 ± 1.1	420	0.093 ± 0.007	441	28 ± 3
MnCo	37.4 ± 0.6	380	0.150 ± 0.006	249	17 ± 6
NiNi	(43.3 ± 0.6) $\times 10^{-3}$	0.44	(2.29 ± 0.14) $\times 10^{-3}$	18.9	82 ± 14
MnNi	(50.5 ± 1.8) $\times 10^{-3}$	0.52	(2.42 ± 0.36) $\times 10^{-3}$	20.9	75 ± 13
MnMn ^c	27.5 ± 0.7	280	0.88 ± 0.35	31.4	1.1 ± 0.4

^a Catalytic proficiency k_{cat}/k_0 with respect to the autohydrolytic constant of $9.8 \times 10^{-8} \text{ s}^{-1}$ determined under the same conditions [10].^b Fluoride inhibition constant.^c The kinetic parameters were determined in the presence of 1.0- μM Mn²⁺ ion.**Table 2**Kinetic parameters for the pH dependence of Leu-pNA and BNPP hydrolysis by MnMn-SgAP.^a

		Leu-pNA	BNPP
k_{cat}	$\text{p}K_{\text{es}1}$	– (6.0)	7.8 ± 0.2 (6.1)
	$\text{p}K_{\text{es}2}$	10.2 ± 0.2 (9.3)	10.0 ± 0.2 (9.6)
k_{cat}/K_m	$\text{p}K_{\text{e}1}$	7.8 ± 0.5 (7.4)	– (5.6)
	$\text{p}K_{\text{e}2}$	9.1 ± 0.2 (9.0)	9.5 ± 0.5 (9.6)

^a The values in parentheses are the ionization constants $\text{p}K_a$ from ZnZn-SgAP catalysis [10].

the activity in the alkaline region of the pH profile of k_{cat} is most likely to be attributed to the ionization of Tyr246 based on the heat of ionization [10]. Moreover, the $\text{p}K_a$ values in the acidic region of the pH profile of k_{cat} for the hydrolysis of BNPP and Leu-pNA are dramatically different, suggesting different mechanisms for the generation of the nucleophile in Leu-pNA and BNPP hydrolysis. Herein, the $\text{p}K_a$ attributed to the nucleophile cannot be obtained from the pH- k_{cat}/K_m plot because the pH profile could not be extended to below pH 7 due to the stability of the di-Mn derivative. Thus, the $\text{p}K_a$ of the nucleophile is at most estimated to be <6.5 (as k_{cat} is still at its peak at pH 7).

3.4. Hydrolysis by homo- and hetero-dinuclear-SgAP

The binding of Zn²⁺, Co²⁺, Cd²⁺, Mn²⁺, or Ni²⁺ to MnE-SgAP activates the enzyme, and the kinetic parameters k_{cat} and K_m for different homo- and hetero-dinuclear derivatives of SgAP toward Leu-pNA and BNPP hydrolysis were determined (Tables 2 and 3).

Table 3Kinetic parameters of homo- and hetero-dinuclear M₁M₂-SgAP toward the hydrolysis of BNPP in 20 mM HEPES at pH 8.0 in the presence of 2 mM CaCl₂.

M ₁ M ₂ -	k_{cat} (s ⁻¹)	CP ^a ($\times 10^9$)	SA ^a	K_m (mM)	k_{cat}/K_m (M ⁻¹ s ⁻¹)
ZnZn [10]	0.45 ± 0.01	41 ^b	154	4.5 ± 0.2	100
MnZn	0.10 ± 0.00	0.91	39.1	3.8 ± 0.3	27
CoCo [9]	0.74 ± 0.02	67 ^b	132	9.5 ± 0.6	78
MnCo	0.084 ± 0.002	0.76	32.2	3.9 ± 0.3	22
NiNi [9]	0.010 ± 0.000	0.091	1.62	10.6 ± 0.4	0.94
MnNi	0.0064 ± 0.0010	0.058	0.87	12.8 ± 0.3	0.50
CdCd [9]	0.043 ± 0.003	0.39	7.55	9.7 ± 2.5	4.4
MnCd	0.016 ± 0.001	0.15	2.50	11.0 ± 1.0	1.42
MnMn ^c	0.081 ± 0.015	0.74	10.4	12.3 ± 1.7	4.67

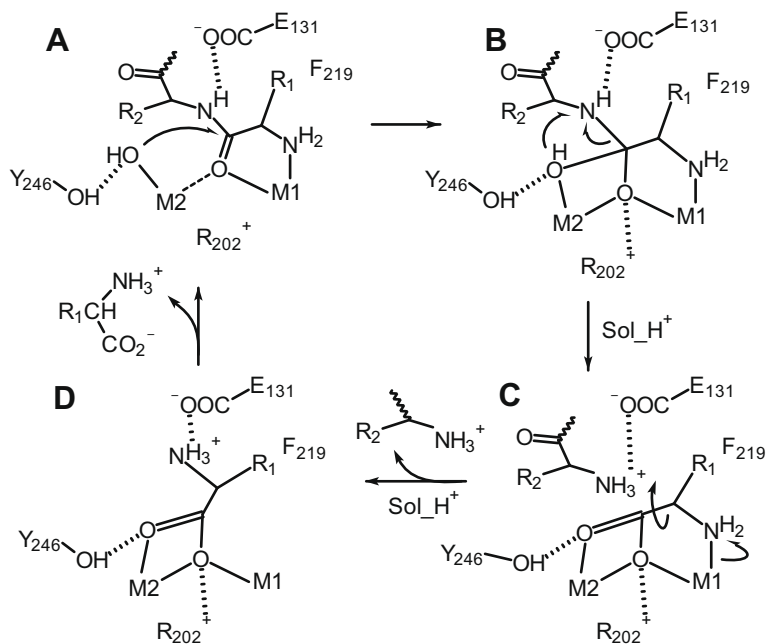
^a CP: Catalytic proficiency k_{cat}/k_0 at pH 8.0 (unless specified) with respect to the autohydrolytic rate constant $k_1 = 1.1 \times 10^{-11} \text{ s}^{-1}$ at pH 7.0 and 25 °C [74] (or 1.1×10^{-10} at pH 8.0, considering OH⁻ as the nucleophile) which is equivalent to a large G^\ddagger value of 138 kJ/mol and a half-life of ~2000 years, or $3.0 \times 10^{-10} \text{ s}^{-1}$ at pH 7.0 and 50 °C [75] and $6.3 \times 10^{-8} \text{ s}^{-1}$ at pH 10.0 and 100 °C [76]. SA: Specific activity (nmol min⁻¹ mg⁻¹) derived from the Michaelis-Menten equation.^b At pH 7 wherein it shows full activity.^c The kinetic parameters were determined in the presence of 1.0- μM Mn²⁺ ion.

There is no detectable exchange between the two metal ions in the derivatives M1M2-SgAP during the measurements since the activities of the derivatives remain the same after a day. The k_{cat} and K_m values are controlled by the second metal M2 toward the hydrolysis of Leu-pNA, e.g., ZnZn- and MnZn-SgAP show similar k_{cat} (101 vs. 92.8 s⁻¹) and K_m (3.27 vs. 3.31 mM) values; whereas MnMn-SgAP affords 27.5 s⁻¹ and 0.875 mM, noticeably different from the values of MnZn-SgAP (Table 1). Likewise, the k_{cat} and K_m values of CdCd- and MnCd-SgAP, CoCo- and MnCo-SgAP, and NiNi- and MnNi-SgAP are comparable to each other, whereas those of MnM2-SgAP are significantly different (Table 1). The results support the significance of M2 in SgAP catalysis.

Comparison of k_{cat} and K_m toward the hydrolysis of BNPP by various M1M2-SgAP is not as clear-cut as in peptide hydrolysis (Table 3). For example, k_{cat} and K_m are 0.45 s⁻¹ and 4.5 mM for ZnZn-SgAP, 0.103 s⁻¹ and 3.76 mM for MnZn-SgAP, and 0.21 s⁻¹ and 12 mM for MnMn-SgAP. Similar results are observed for the pairs of Co²⁺, Cd²⁺, and Ni²⁺ derivatives, wherein k_{cat} and K_m are significantly affected by both metal ions, as opposed to the case of Leu-pNA hydrolysis where M2 plays a more significant role in catalysis and substrate binding (Table 1). The results suggest that the mechanisms for peptide hydrolysis and BNPP hydrolysis are different, with M2 showing more influence on Leu-pNA hydrolysis than on BNPP hydrolysis.

3.5. Mechanism for peptide hydrolysis

The mechanisms for peptide hydrolysis by ApAP, *E. coli* Met AP, and bILAP vary from mononuclear to dinuclear peptide hydrolysis; however, a few other APs show that both metal ions are required for TS[‡] stabilization and catalysis [19–25,29–35]. On the basis of the results presented here, a dinuclear mechanism is proposed for SgAP (Scheme 1, Fig. 6).



Scheme 1.

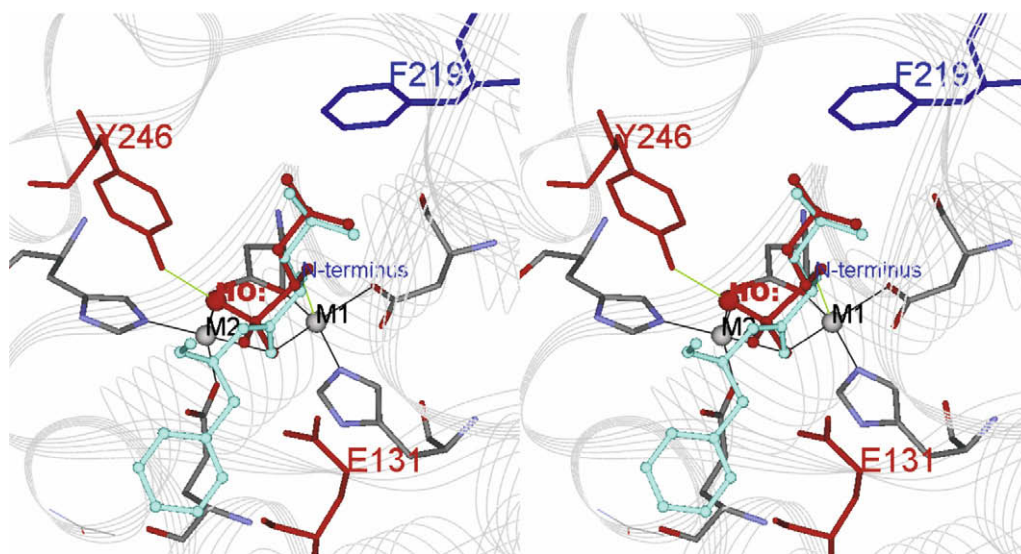


Fig. 6. Relaxed-eye stereo plot of plausible binding modes for a peptide substrate (cyan; Leu-Phe) and a TS^\ddagger analogue (α -aminoisopentylphosphate; red ball-and-stick structure) in the active site of SgAP. The bound inhibitor is obtained from the crystal structure of bILAP which is superimposed onto the dinuclear center of SgAP and show appropriate hydrophobic interaction. Then the substrate is superimposed onto the TS^\ddagger inhibitor to reveal its interaction with the hydrophobic site and the metal center. The N-terminal amino group and the nucleophilic water (red sphere) are as labeled.

3.5.1. Binding mode of peptide substrate

There are three functional groups in the substrate which can potentially interact with SgAP [19–25,29–35]: the carbonyl of the scissile peptide bond with M1 (and a dipole–charge interaction with M2), the amino terminus with M1, and the hydrophobic side chain with Phe219 (Scheme 1A). To visualize substrate and inhibitor binding to SgAP, the TS^\ddagger analogue α -aminoalkylphosphonate and the active-site metal ions from the EI complex of bILAP [3] are superimposed onto the active center of SgAP (red ball-and-stick structure; Fig. 6) which reveals that the inhibitor binding modes of these two enzymes are similar, wherein the N-terminal hydrophobic residue is pointing toward Phe219 in SgAP (blue; Fig. 6) and the

amino group of the TS^\ddagger analogue is within bonding distance to M1. A substrate (Leu-Phe) is superimposed onto the bound inhibitor in the active site of SgAP in order to reveal a possible substrate binding configuration (cyan; Fig. 6).

There are two possible orientations for the substrate to bind to the active-site metal ions [10]: (a) The scissile carbonyl group is bound to M1 (and M2 via charge–dipole interaction) which mimics the bridging oxygen of the bound α -aminoalkylphosphonate inhibitor or (b) the carbonyl group is in place of the inhibitor oxygen that is H-bonded to the Tyr246. In the former case, the carbonyl oxygen is bound to M1 at the favorable syn position with the peptide bond facing the plausible nucleophile on M2 (see below),

whereas the substrate is in an unfavorable binding situation in the latter case with the metal situated off the syn or anti position of the scissile carbonyl oxygen.

3.5.2. Nucleophile in peptide hydrolysis

The substrate binding mode Section 3.5.1 discussed above renders the coordinated water that is H-bonded to Tyr246 (red HO; Fig. 6) to situate on one side of the scissile peptide bond to perform nucleophilic attack (Scheme 1A). Crystal structure study of this enzyme suggests that Tyr246 is involved in H-bonding with a plausible coordinated water at the position of one oxygen of a coordinated dibasic phosphate. The role of Tyr246 as a general acid thus can further enhance the Lewis acidity of the water, resulting in lowering in the pK_a and increasing in the nucleophilicity of the water for effective nucleophilic attack. The role of a general acid to lower the pK_a and enhance the nucleophilicity of a coordinated water and a Cys nucleophile, respectively, was also proposed in the case of metallonucleases [54,55] and glutaredoxin [56]. The crystal structures of several dinuclear hydrolytic enzymes with a metal-metal distance 3.5 Å reveal a bridging hydroxide which has been proposed to be the nucleophile or the precursor of the nucleophile, e.g., ApAP [46], some PAP [57], urease [58], and pyrophosphatase [59]. If this would be the case in SgAP, both metal ions should influence the activity; which is not the case. The uncompetitive inhibition of F^- suggests that metal-bond nucleophilic OH^- becomes available for replacement by F^- only upon substrate binding. The substrate binding mode described herein suggests that the bridging OH^- is replaced by the bound substrate. This binding may induce changes in the active site and proper orientation of the scissile peptide bond relative to the attacking nucleophile. The F^- inhibition constants are significantly influenced by the second metal ion M2, indicating that the nucleophilic coordinated water is on M2.

Glu131 may further activate the nucleophile and/or stabilize the TS^\ddagger [49], analogues to Glu270 in carboxypeptidase A which is also involved in deprotonation of the nucleophile and protonation of the amino terminus of the leaving group [60]. The pH profile of F^- inhibition reveals a pK_a at 9.3 which may be attributable to Tyr246, and is consistent with its role in the interaction and proper orientation of the nucleophile as proposed in accordance with crystal structures. It is thus most likely that the “first metal” is near the hydrophobic site (i.e., M1 in Fig. 6) while M2 hosts the nucleophilic water that is H-bonded to Tyr246 and facing the scissile $-CO-NHR-$ plane. Nucleophilic attack by this water affords the TS^\ddagger as in the structure of bILAP with a bound TS^\ddagger analogue (red ball-and-stick structure, Fig. 6 and Scheme 1B).

3.5.3. Stabilization of the TS^\ddagger

The kinetic results suggest that M2 plays a major role in stabilizing TS^\ddagger and performing nucleophilic attack since k_{cat} varies more with this metal ion. However, the crystal structure of bILAP with a bound TS^\ddagger -like α -aminoalkylphosphate inhibitor [3] shows that both metal ions are involved in TS^\ddagger binding and stabilization (Fig. 6). Upon nucleophilic attack, the oxygen on the scissile carbonyl group changes from sp^2 hybridization to sp^3 hybridization in the *gem*-dilute-like intermediate which allows the oxygen to serve as a better bridging ligand between the two metals. The pH dependence of k_{cat} toward the hydrolysis of Leu-pNA by different metal derivatives of SgAP shows a pK_a value of ~ 9.2 , assignable to Tyr246 (near M2) which is suggested to activate the nucleophilic water and stabilize the *gem*-dilute-like TS^\ddagger . The results from phosphate inhibition toward the hydrolysis of Leu-pNA by native and phenylglyoxal-modified ZnZn-SgAP and from NMR relaxation studies of Co^{2+} derivatives suggest that Arg202 may also be involved in TS^\ddagger stabilization [41] (Scheme 1B).

3.5.4. Release of the products

The TS^\ddagger breaks down (Scheme 1C) to release the C-terminal main protein body, while the N-terminal amino acid presumably remains bound (Scheme 1D) as suggested by crystallographic studies of various amino acid-bound SgAP [61]. The N-terminal amino group is supposed to detach from the metal after the substrate is hydrolyzed owing to increase in its pK_a after bond cleavage (Scheme 1C). Crystal structures of SgAP with a bound amino acid (Met, Leu, or Phe) show that one carboxyl oxygen of the bound amino acid is coordinated to M2 and H-bonded to Tyr246 while the other oxygen binds to both metal ions [61]. Moreover, the amino group of the bound amino acid product is detached from M1, and is presumably H-bonded to Glu131 (Scheme 1C and D). The pH profile for Leu inhibition toward Leu-pNA hydrolysis shows a weak inhibition and no clear pK_a value at pH 6.0 to 10.0 [10]. The release of the amino acid product can thus spontaneously occur without the assistance of a general acid.

3.6. Catalytic promiscuity

Dinuclear hydrolases such as APs have been investigated by numerous methods to reveal the reaction mechanisms [6,45,62,63], e.g., the role of metal ions in activity [19,31,64], and stabilization of the tetrahedral TS^\ddagger , and binding of TS^\ddagger -inhibitors [3,65]. Although a phospho-center has been known to serve as a TS^\ddagger analogue of peptide substrates, the phosphodiester BNPP and the phosphonate ester *p*-nitrophenylphenylphosphonate can be effectively hydrolyzed by SgAP and its metal derivatives with a catalytic proficiency of ~ 40 billion-fold for the native enzyme and 67 billion-fold for the di- Co^{2+} derivative toward BNPP hydrolysis under physiological conditions [9,10]. Moreover, CuCu-SgAP exhibits a significant catechol oxidase activity, showing $\sim 10\%$ catalytic efficiency compared to a native catechol oxidase [40]. Revealing the key factors involved in these alternative catalyses are essential to gain further insight into dinuclear catalysis as well as “enzyme catalytic promiscuity [66–70]”.

The catalytic proficiencies in terms of the first-order rate constants [71,72] (i.e., k_{cat}/k_1 with k_1 the uncatalyzed rate constant) for Leu-pNA hydrolysis by the several metal-substituted derivatives of SgAP at pH 8.0 are quite significant, ranging from 0.44×10^6 for the di-Ni derivative to 6.7×10^9 for the native enzyme with respect to k_1 of $9.8 \times 10^{-8} s^{-1}$ determined under the same conditions (Table 1), but are much smaller for the less specific peptide substrates [10]. The k_{cat}/k_1 value for Leu-pNA hydrolysis by the native enzyme represents an enormous G^\ddagger value of -57 kJ/mol at 303 K. These values of catalytic proficiency for peptide hydrolysis serve as the criteria for the evaluation of the promiscuous catalysis toward BNPP hydrolysis.

Phosphoesters resembles the *gem*-dilute-like TS^\ddagger of peptides during hydrolysis, which explains why BNPP can serve as an inhibitor toward peptide hydrolysis by SgAP and ApAP [9,10]. Moreover, BNPP and a few phosphoesters and fluorophosphates are also known to be TS^\ddagger -inhibitors against serine proteases and esterases such as trypsin, chymotrypsin, and acetylcholine esterase through covalent linkage with the nucleophilic serine in the active site [7,11–13] to afford $Ser-O-P(O)_2^-OR$ with concomitant cleavage of a phosphoester or the P-F bond that resembles the “initial burst” kinetics of serine proteases. However, the phosphoester $Ser-O-P(O)_2^-OR$ is indefinitely stable, thus has only one turn-over for the phosphoester bond cleavage by these enzymes. On the other hand, sulfonamide bond cleavage by subtilisin is a novel observation of catalytic promiscuity in the serine protease family [73]. Likewise, the cleavage of BNPP by SgAP and its metal derivatives is also catalytic with enormous catalytic proficiencies relative to the autohydrolytic rate constant [74–76] (Table 3). The second-order rate constants of BNPP hydrolysis by SgAP and its

metal derivatives (100 and $0.5\text{--}78\text{ M}^{-1}\text{ s}^{-1}$, respectively) are considerably higher than those of many synthetic chemical model systems of Zn^{2+} complexes (e.g., in the range of $k_2 \sim 10^{-6}$ to $10^{-4}\text{ M}^{-1}\text{ s}^{-1}$) and other chemical systems performed at $>35\text{ }^\circ\text{C}$ and $>\text{pH } 8.5$ [77–85]. Thus, the high activity of SgAP cannot simply be attributed to the high Lewis acidity of the metal ions as in the chemical model systems. The activities of SgAP and its metal derivatives toward BNPP hydrolysis are significantly higher than or comparable to those of some native phosphoester-hydrolyzing enzymes and their derivatives, such as alkaline phosphatase ($0.05\text{ M}^{-1}\text{ s}^{-1}$ [86]) and *Burkholderia* phosphonate monoester hydrolase ($11.4\text{ M}^{-1}\text{ s}^{-1}$ [87]) and ethyl(*p*-nitrophenyl)phosphate hydrolysis by metal derivatives of *Pseudomonas* phosphotriesterase ($1.1\text{--}7.2\text{ M}^{-1}\text{ s}^{-1}$ [88]). The specific activities toward the hydrolysis of 1.0 mM BNPP by SgAP and its derivatives ($0.87\text{--}154\text{ nmol min}^{-1}\text{ mg}^{-1}$ derived from Table 3) are also in the range of those of several phosphodiesterases and phosphatases ($0.3\text{--}2450$ and $\sim 2\text{--}40\text{ nmol min}^{-1}\text{ mg}^{-1}$, respectively) [89,90]. However, native phosphodiester-specific enzymes can have much higher activities, such as the phosphodiesterase gene product of *ElaC* shows k_{cat} of 59 s^{-1} and $k_{\text{cat}}/K_{\text{m}} = 1480\text{ M}^{-1}\text{ s}^{-1}$ [91]. Nevertheless, this comparison concludes that the phosphodiesterase activity of SgAP and derivatives toward BNPP hydrolysis are indeed quite significant.

3.7. Mechanism for BNPP hydrolysis

The hydrolysis of phosphoesters has different mechanistic requirements from peptide hydrolysis, e.g., a tetrahedral *gem*-diolate-like TS^\ddagger for the former and a trigonal bipyramidal TS^\ddagger for the latter. On the basis of the different (a) influences by M1 and M2, (b) inhibition patterns, (c) pH-activity profiles, and (d) pK_a values between BNPP and peptide hydrolysis by SgAP, we propose a mechanism for the proficient BNPP hydrolysis below (Scheme 2), wherein BNPP is bound to the active site analogous to the TS^\ddagger of peptide during hydrolysis.

3.7.1. Binding mode of BNPP

The variation in the k_{cat} and K_{m} values among SgAP derivatives on BNPP hydrolysis (Table 3) indicates the hydrolytic reaction is influenced by both M1 and M2. M2 plays a significant role in pep-

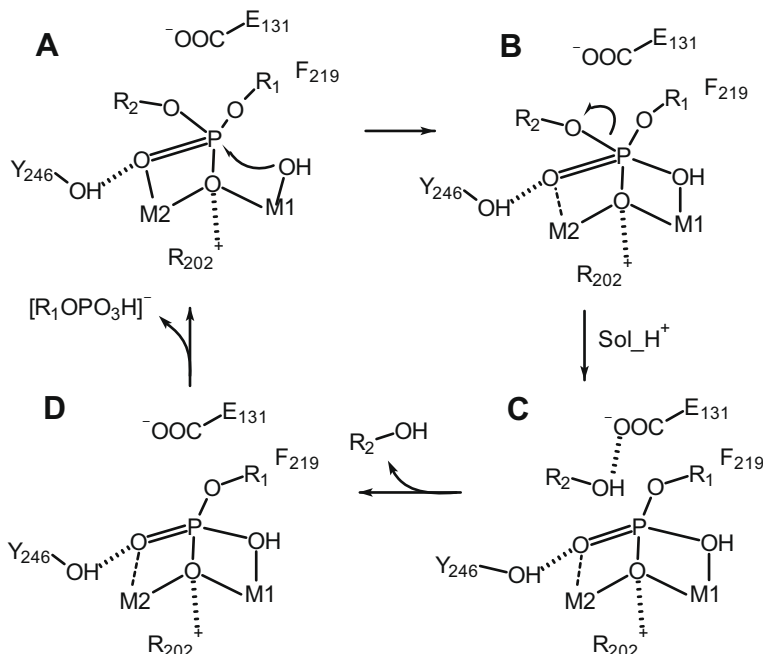
ptide hydrolysis, but is shown herein to have a different role in BNPP hydrolysis. The binding mode of BNPP is proposed to be similar to the TS^\ddagger in peptide hydrolysis (cyan; Fig. 7) where two oxygens of phosphoester bind to M2 with one bridging to M1 (cf. red ball-and-stick inhibitor in Fig. 6; Scheme 2A). Phosphate inhibits BNPP and Leu-*p*NA hydrolysis in competitive and noncompetitive patterns, respectively, thus it competes with BNPP binding to SgAP, but not with Leu-*p*NA. The combination of the pH profiles, kinetic, and ^{31}P NMR relaxation studies suggests that phosphate binds to Arg202 [16,34,41]. This Arg is supposed to bind the TS^\ddagger in Leu-*p*NA hydrolysis, and should bind the TS^\ddagger -like BNPP (Scheme 2A). In addition, the similar pK_a values for BNPP and Leu-*p*NA hydrolysis at the alkaline side indicates the involvement of the same amino acid for catalysis and/or TS^\ddagger stabilization, suggested to be Tyr246.

3.7.2. Generation of nucleophile

The different F^- inhibition patterns toward BNPP (no inhibition) and Leu-*p*NA (uncompetitive) hydrolysis reflect different mechanisms for the generation of the nucleophile in these two hydrolytic reactions. In addition, the steric hindrance imposed by the active site on the leaving group and the requirement of an in-line attack on phosphoester substrates [92,93] by the nucleophile during hydrolysis suggest that M1 may possess the nucleophile (red HO $^-$; in Fig. 7; Scheme 2A) and the leaving group is near the opening of the active site (i.e., the group on the left-hand side of the substrate, Fig. 7). The nucleophile in the peptide hydrolysis is integrated into the substrate at the TS^\ddagger , thus is not available for the hydrolysis of the TS^\ddagger -like BNPP, which as a consequence must have a different nucleophile.

3.7.3. Stabilization of the TS^\ddagger

The pH dependence of k_{cat} is controlled by a pK_a value of 9.2, suggested to be due to Tyr246. The k_{cat} and K_{m} values of BNPP hydrolysis by SgAP are dependent on both metal ions, indicating both metal ions are involved in BNPP hydrolysis. Since phosphate and fluoride inhibitions indicate that BNPP binds to SgAP as a TS^\ddagger analogue of a peptide substrate (red inhibitor in Fig. 6), and the nucleophile is expected to be generated by M1 (:OH in Fig. 7) rather than M2 in peptide hydrolysis since the nucleophile in pep-



Scheme 2.

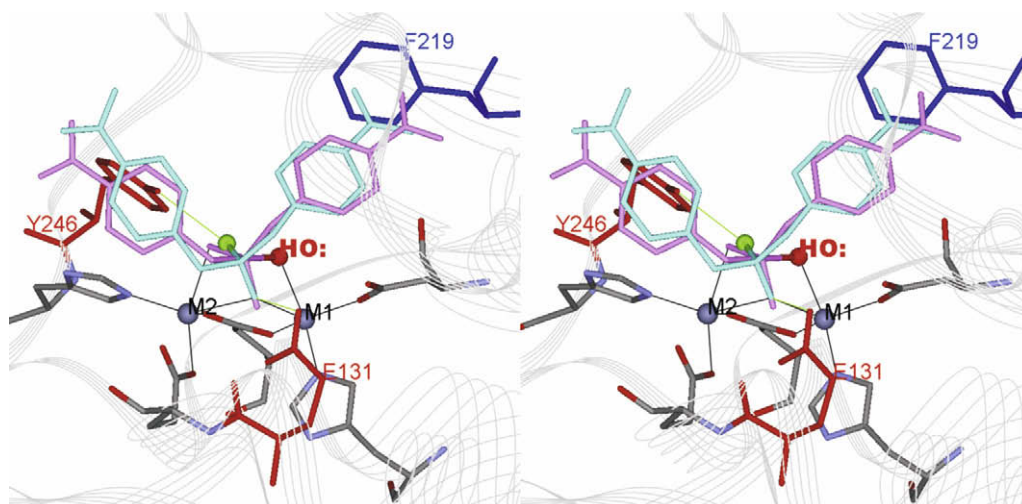


Fig. 7. Relaxed-eye stereo plot of plausible binding of BNPP (cyan) and its TS[‡] (pink) docked into the active site of SgAP. The configuration of the TS[‡] is arranged to adopt a trigonal bipyramidal geometry with one apex occupied by the nucleophilic water (HO:, red sphere) that is *trans* to the leaving group (on the left) after in-line attack at the phospho-center. The nucleophilic water in peptide hydrolysis is labeled as a green sphere.

tide hydrolysis is now part of the TS[‡]. This nucleophile is able to perform S_N2 in-line attack [92,93] in BNPP hydrolysis from the opposite site of the leaving group to form a trigonal bipyramidal TS[‡] (pink; Fig. 7). Herein, Arg202 was suggested to stabilize the TS[‡] (whereas a counterpart is not present in ApAP), along with Tyr246, Glu131, and both metal ions (Scheme 2B).

3.7.4. The release of the products

The phosphomonoester product has been shown to be a good inhibitor toward BNPP hydrolysis ($K_i = 0.9$ mM) [10]. Thus, upon detachment of the leaving group *p*-nitrophenol (Scheme 2C), an enzyme–product complex is formed which adopts a configuration analogous to the bound phosphate in the enzyme [16] with one O originated from the nucleophile bound to M1, one bridging O, and the other one H-bonded with Tyr246 and may bind to M2 (Scheme 2D). Release of the phosphomonoester and placement of coordination sphere with water molecules complete the catalytic cycle.

4. Concluding remarks

Although enzymes are frequently ascribed to possess catalytic specificity, most enzymes are known to catalyze the conversion of a family of substrates and analogues with similar structures, such as the hydrolysis of peptides and carboxylesters by peptidases. Several enzymes have also been demonstrated to perform catalyses toward substrates of different families, exhibiting enzyme catalytic promiscuity [66–70]. However, it would be less expected for an enzyme to exhibit an enormous alternative catalysis that is normally carried out by an evolutionarily and structurally unrelated enzyme. We describe in this report the hydrolysis of a phosphodiester substrate by SgAP and its metal derivatives, reaching a dramatic 67-billion-fold rate enhancement relative to the non-catalyzed reaction at neutral pH and room temperature and having rate constants comparable to several native phosphoester-hydrolyzing enzymes.

Dinuclear centers of various metal ions are found in many hydrolytic enzymes, including urease (Ni), nucleases (Zn), arginase (Mn), prolidase (Mn), and AP (Zn or Co) [6], as well as in a number of Fe-, Mn-, and Cu-containing oxidases and oxygenases [94]. The catalytic versatility of dinuclear SgAP and its metal derivatives entitle this enzyme to serve as a “natural dinuclear model system

[9]” for further investigation of various dinuclear catalyses. Indeed, the di-Cu derivative of SgAP has recently been demonstrated to exhibit a significant activity toward the oxidation of catechol and derivatives [40], despite its very different active-site structure from that of catechol oxidase. Future studies of this unique natural dinuclear model system by means of physical methods and molecular biology are expected to provide further information to gain better understanding of various dinuclear catalyses in chemical and biological systems and further knowledge about how to use this and other metalloenzymes as scaffolds to build artificial metalloenzymes of novel catalytic activities.

5. Abbreviations

AP	aminopeptidase
ApAP	<i>Aeromonas proteolytica</i> AP
bLAP	Leu-specific AP from bovine lens
BNPP	bis(<i>p</i> -nitrophenyl)phosphate
DEAE	diethylaminoethyl
HEPES	N-[2-hydroxyethyl] piperazine-NN-2-ethanesulfonic acid
MES	2-[N-morpholino]ethanesulfonic acid
PAP	purple acid phosphatase
pkLAP	Leu-specific AP from porcine kidney
<i>p</i> NA	<i>p</i> -nitroanilide
SgAP	<i>Streptomyces griseus</i> aminopeptidase
TS [‡]	transition-state

Acknowledgments

This work was supported by the Petroleum Research Funds administrated by the American Chemical Society (ACS-PRF #35313-AC3) and by the National Institutes of Health (GM064400-01A2).

References

- [1] L. Pauling, Chemical achievement and hope for the future, *Am. Sci.* 36 (1948) 51–58.
- [2] R.A. Lerner, S.J. Benkovic, P.J. Schultz, At the crossroad of chemistry and immunology: catalytic antibodies, *Science* 252 (1991) 659–667.
- [3] N. Strater, W.N. Lipscomb, Transition state analogue L-leucinephosphonic acid bound to bovine lens leucine aminopeptidase: X-ray structure at 1.65 Å resolution in a new crystal form, *Biochemistry* 34 (1995) 9200–9210.

- [4] B. Lejczak, P. Kafarski, J. Zygmunt, Inhibition of aminopeptidases by aminophosphonates, *Biochemistry* 28 (1989) 3549–3555.
- [5] D. Tronrud, A.F. Monzingo, B.W. Matthews, Crystallographic structural analysis of phosphoramidates as inhibitors and transition-state analogs of thermolysin, *Eur. J. Biochem.* 157 (1986) 261–268.
- [6] W.N. Lipscomb, N. Strater, Recent advances in zinc enzymology, *Chem. Rev.* 96 (1996) 2375–2433.
- [7] C.B. Millard, G. Kryger, A. Ordentlich, H.M. Greenblatt, M. Harel, M.L. Raves, Y. Segal, D. Garak, A. Shafferman, I. Silman, J.L. Sussman, Crystal structures of aged phosphonylated AChE: nerve agent reaction product at the atomic level, *Biochemistry* 38 (1999) 7032–7039.
- [8] H.I. Park, L.-J. Ming, A novel 10^{10} Rate enhancement of phosphodiester hydrolysis by a dinuclear aminopeptidase—transition-state analogues as substrates?, *Angew Chem. Intl. Ed. Engl.* 111 (1999) 3097–3100.
- [9] A. Ercan, H.I. Park, L.-J. Ming, Enormous enhancement of the hydrolyses of phosphoesters by dinuclear centers: *Streptomyces* aminopeptidase as a “natural model system”, *Chem. Commun.* (2000) 2501–2502.
- [10] A. Ercan, H.I. Park, L.-J. Ming, A “moonlighting” dizinc aminopeptidase from *Streptomyces griseus*: mechanism for peptide hydrolysis and 4×10^{10} -fold acceleration of the alternative phosphoester hydrolysis, *Biochemistry* 45 (2006) 13779–13793.
- [11] K. Nishida, Y. Ohta, M. Ito, Y. Nagamura, S. Kitahara, K. Fujii, I. Ishihuro, Conversion of β -glutamylcysteinylethyl ester to glutathione in rat hepatocytes, *Biochim. Biophys. Acta.* 1313 (1996) 47–53.
- [12] C.V. Preuss, C.V. Svensson, Arylacetamide deacetylase activity towards monoacetyldapsone. Species comparison, factors that influence activity, and comparison with 2-acetylaminofluorene and *p*-nitrophenyl acetate hydrolysis, *Biochem. Pharmacol.* 51 (1996) 1661–1668.
- [13] L. Luan, T. Sugiyama, S. Takai, T. Adachi, Y. Katagiri, K. Hirano, Purification and characterization of pranlukast hydrolase from rat liver microsomes: the hydrolase is identical to carboxylesterase pf 6.2, *Biol. Pharm. Bull.* 20 (1997) 71–75.
- [14] A. Spungin, S. Blumberg, *Streptomyces griseus* aminopeptidase is a calcium-activated zinc metalloprotein purification and properties of the enzyme, *Eur. J. Biochem.* 183 (1989) 471–477.
- [15] R. Gilboa, A. Spungin-Bialik, G. Wohlfart, D. Schomburg, S. Blumberg, G. Shoham, Interaction of *Streptomyces griseus* aminopeptidase with amino acid reaction products and their implications toward a catalytic mechanism, *Proteins: Struct. Func. Genet.* 44 (2001) 490–504.
- [16] H.M. Greenblatt, O. Almog, B. Maras, A. Spungin-Bialik, D. Barra, S. Blumberg, G. Shoham, *Streptomyces griseus* aminopeptidase: X-ray crystallographic structure at 1.75 Å resolution, *J. Mol. Biol.* 265 (1997) 620–636.
- [17] R. Gilboa, A. Spungin-Bialik, G. Wohlfahrt, D. Schomburg, S. Blumberg, G. Shoham, Interactions of *Streptomyces griseus* aminopeptidase with amino acid reaction products and their implications toward a catalytic mechanism, *Proteins* 44 (2001) 490–504.
- [18] B. Chevrier, C. Schalk, H. D’Orchymont, J.-M. Rondeau, D. Moras, C. Tarnus, Crystal structure of *Aeromonas proteolytica* aminopeptidase: a prototypical member of the co-catalytic zinc enzyme family, *Structure* 2 (1994) 283–291.
- [19] R.C. Holz, The aminopeptidase from *Aeromonas proteolytica*: structure and mechanism of co-catalytic metal centers involved in peptide hydrolysis, *Coord. Chem. Rev.* 232 (2002) 5–26.
- [20] N.J. Cospier, V. D’Souza, R. Scott, R.C. Holz, Structural evidence that the methionyl aminopeptidase from *Escherichia coli* is a mononuclear metalloprotease, *Biochemistry* 40 (2001) 13302–13309.
- [21] G.S. Cottrell, N.M. Hooper, A.J. Turner, Cloning, expression and characterization of human cytosolic aminopeptidase P: a single manganese(II)-dependent enzyme, *Biochemistry* 3 (2000) 15121–15128.
- [22] J.M. Prescott, F.W. Wagner, *Biochemistry* 24 (1985) 5350–5356.
- [23] L.-Y. Lin, H.I. Park, L.-J. Ming, Metal-binding and active-site structure of di-zinc *Streptomyces griseus* aminopeptidase, *J. Biol. Inorg. Chem.* 2 (1997) 744–749.
- [24] C. Hasselgren, H.I. Park, L.-J. Ming, Metal ion binding and activation of *Streptomyces griseus* dinuclear aminopeptidase: cadmium(II) as a model, *J. Biol. Inorg. Chem.* 6 (2001) 120–127.
- [25] M.N. Harris, L.-J. Ming, Different phosphate binding modes of *Streptomyces griseus* aminopeptidase between crystal and solution states and the status of zinc-bound water, *FEBS Lett.* 455 (1999) 321–324.
- [26] M.Y. Chae, G.A. Omburo, P.A. Lindahl, F.M. Raushel, Utilization of copper as a paramagnetic probe for the binuclear metal center of phosphotriesterase, *Arch. Biochem. Biophys.* 316 (1995) 765–772.
- [27] S.B. Hong, F.M. Raushel, Metal–substrate interactions facilitate the catalytic activity of the bacterial phosphotriesterase, *Biochemistry* 35 (1996) 10904–10912.
- [28] I. Bertini, C. Luchinat, The reaction pathways of zinc enzyme and related biological catalysts, in: I. Bertini, H.B. Gray, S.J. Lippard, J.S. Valentine (Eds.), *Bioinorganic Chemistry*, University Science Books, Sausalito, CA, 1994, pp. 37–106.
- [29] M.P. Allen, A.H. Yamada, F.H. Carpenter, Kinetic parameters of metal-substituted leucine aminopeptidase from bovine lens, *Biochemistry* 22 (1983) 3778–3783.
- [30] H.E. Van Wart, S.H. Lin, Metal binding stoichiometry and mechanism of metal ion modulation of porcine kidney leucine aminopeptidase, *Biochemistry* 20 (1981) 5682–5689.
- [31] J.M. Prescott, F.W. Wagner, B. Holmquist, B.L. Vallee, One hundred fold increased activity of *Aeromonas* aminopeptidase by sequential substitutions with Ni^{2+} or Cu^{2+} followed by Zn^{2+} , *Biochem. Biophys. Res. Commun.* 114 (1983) 646–652.
- [32] M.E. Bayliss, J.M. Prescott, Modified activity of *Aeromonas* aminopeptidase: metal ion substitutions and role of substrate, *Biochemistry* 25 (1986) 8113–8117.
- [33] J.M. Prescott, F.W. Wagner, B. Holmquist, B.L. Vallee, Spectral and kinetic studies of metal-substituted *Aeromonas* aminopeptidase: Nonidentical, interacting metal-binding sites, *Biochemistry* 24 (1985) 5350–5356.
- [34] B. Bennett, R.C. Holz, Spectroscopically distinct cobalt(II) sites in heterodimetallic forms of the aminopeptidase from *Aeromonas proteolytica*: characterization of substrate binding, *Biochemistry* 36 (1997) 9837–9846.
- [35] B. Bennett, R.C. Holz, EPR studies on the mono- and di-cobalt-substituted forms of the aminopeptidase from *Aeromonas proteolytica*. Insight into the catalytic mechanism of dinuclear hydrolases, *J. Am. Chem. Soc.* 119 (1997) 1923–1933.
- [36] C.C. De Paola, B. Bennett, R.C. Holz, D. Ringe, G.A. Petsko, 1-Butaneboric acid binding to *Aeromonas proteolytica* aminopeptidase: a case of arrested development, *Biochemistry* 38 (1999) 9048–9053.
- [37] G.N. La Mar, W.DeW. Horrocks, R.H. Holm (Eds.), *NMR of Paramagnetic Molecules*, Academic, NY, 1973.
- [38] I. Bertini, C. Luchinat, *NMR of Paramagnetic Molecules in Biological Systems*, Benjamin/Cumming, Menlo Park, CA, 1986.
- [39] L.-J. Ming, in: L. Que (Ed.), *Physical Methods in Bioinorganic Chemistry*, Spectroscopy and Magnetism, University Science Books, CA, 2000, pp. 375–464.
- [40] G.F.Z. da Silva, L.-J. Ming, Catechol oxidase activity of di- Cu^{2+} -substituted aminopeptidase from *Streptomyces griseus*, *J. Am. Chem. Soc.* 127 (2005) 16380–16381.
- [41] M.N. Harris, C. Bertolucci, L.-J. Ming, Paramagnetic cobalt(II) as a probe for kinetic and NMR relaxation studies of phosphate binding and the catalytic mechanism of *Streptomyces* dinuclear aminopeptidase, *Inorg. Chem.* 41 (2002) 5582–5588.
- [42] M.W.H. Pinke, M. Merx, B.A. Averill, Fluoride inhibition of bovine spleen purple acid phosphatase: Characterization of a ternary enzyme–phosphate–fluoride complex as a model for the active enzyme–substrate–hydroxide complex, *Biochemistry* 38 (1999) 9926–9936.
- [43] N.E. Dixon, R.L. Blakeley, B. Zerner, Jack bean urease (EC 3.5.1.5). III. The involvement of active-site nickel ion in inhibition by β -mercaptoethanol, phosphoramidate, and fluoride, *Can. J. Biochem.* 58 (1980) 481–488.
- [44] M.J. Todd, R.P. Hausinger, Fluoride inhibition of *Klebsiella aerogenes* urease: mechanistic implications of a pseudo-uncompetitive slow-binding inhibitor, *Biochemistry* 39 (2000) 5389–5396.
- [45] G. Schenk, L.R. Gahan, L.E. Carrington, N. Mitic, M. Valizadeh, J. De Jersey, L.W. Guddat, Phosphate forms an unusual tripod complex with the Fe–Mn center of sweet potato purple acid phosphatase, *Proc. Nat. Acad. Sci. USA* 102 (2005) 273–278.
- [46] G. Chen, T. Edwards, V.M. D’Souza, R.C. Holz, Mechanistic studies on the aminopeptidase from *Aeromonas proteolytica*: a two-metal ion mechanism for peptide hydrolysis, *Biochemistry* 36 (1997) 4278–4286.
- [47] A. W.J.W. Tepper, L. Bubacco, G.W. Canters, Structural basis and mechanism of the inhibition of the type-3 copper protein tyrosinase from *Streptomyces antibioticus* by halide ions, *J. Biol. Chem.* 277 (2002) 30436–30444.
- [48] J.O. Baker, J.M. Prescott, *Aeromonas* aminopeptidase: pH dependence and a transition-state-analogue inhibitor, *Biochemistry* 22 (1983) 5322–5331.
- [49] Y.F. Hershovitz, R. Gilboa, V. Reiland, G. Shoham, Y. Shoham, Catalytic mechanism of SGAP, a double-zinc aminopeptidase from *Streptomyces griseus*, *FEBS J.* 274 (2007) 3864–3876.
- [50] D.S. Auld, B.L. Vallee, Kinetics of carboxypeptidase A. pH dependence of tripeptide hydrolysis catalyzed by zinc, cobalt, and manganese enzymes, *Biochemistry* 9 (1970) 4352–4359.
- [51] M. Izquierdo-Martin, R.L. Stein, Mechanistic studies on the inhibition of thermolysin by a peptide hydroxamic acid, *J. Am. Chem. Soc.* 114 (1992) 325–331.
- [52] H.I. Park, L.-J. Ming, Mechanistic studies of the astacin-like serrata metalloendopeptidase serralyisin: Highly active (>2000%) Co(II)- and Cu(II)-substituted derivatives for further corroboration of a “metallotriad” mechanism, *J. Biol. Inorg. Chem.* 7 (2002) 600–610.
- [53] N. Strater, W.N. Lipscomb, Two-metal ion mechanism of bovine lens leucine aminopeptidase: Active site solvent structure and binding mode of L-leucinal, a gem-diolate transition state analog, by X-ray crystallography., *Biochemistry* 34 (1995) 14792–14800.
- [54] N.C. Horton, B.A. Connolly, J.J. Perona, Inhibition of EcoRV endonuclease by deoxyribo-3'-S-phosphorothiolates: a high-resolution X-ray crystallographic study, *J. Am. Chem. Soc.* 122 (2000) 3314–3324.
- [55] N.C. Horton, K.J. Newberry, J.J. Perona, Metal ion-mediated substrate-assisted catalysis in type II restriction endonucleases, *Proc. Natl. Acad. Sci. USA* 95 (1998) 13489–13494.
- [56] S.C. Jao, S.M.E. Ospina, A.J. Berdis, D.W. Starke, C.B. Post, J.J. Mieyal, Computational and mutational analysis of human glutaredoxin (thioltransferase): Probing the molecular basis of the low pK(a) of cysteine 22 and its role in catalysis, *Biochemistry* 45 (2006) 4785–4796.
- [57] E.G. Funhoff, T.E. de Jongh, B.A. Averill, Direct observation of multiple protonation states in recombinant human purple acid phosphatase, *J. Biol. Inorg. Chem.* 10 (2005) 550–563.

- [58] M.J. Todd, R.P. Hausinger, Fluoride inhibition of *Klebsiella aerogenes* urease: mechanistic implications of a pseudo-uncompetitive, slow-binding inhibitor, *Biochemistry* 39 (2000) 5389–5396.
- [59] P. Pohjanjoki, I.P. Fabrichniy, V.N. Kasho, B.S. Cooperman, A. Goldman, A.A. Baykov, R. Lahti, Probing essential water in yeast pyrophosphatase by directed mutagenesis and fluoride inhibition measurements, *J. Biol. Chem.* 276 (2001) 434–441.
- [60] D.W. Christianson, W.N. Lipscomb, Carboxypeptidase A, *Accounts Chem. Res.* 22 (1989) 62–69.
- [61] R. Gilboa, H.M. Greenblatt, M. Perach, A. Spungin-Bialik, U. Lessel, G. Wohlfahrt, D. Schomburg, S. Blumberg, G. Shoham, Interactions of *Streptomyces griseus* aminopeptidase with a methionine product analogue: a structural study at 1.53 Å resolution, *Acta Crystallog. D* 56 (2000) 551–558.
- [62] D.W. Christianson, J.D. Cox, Catalysis by metal-activated hydroxide in zinc and manganese metalloenzymes, *Ann. Rev. Biochem.* 68 (1999) 33–57.
- [63] H. Kim, W.N. Lipscomb, Structure and mechanism of bovine lens leucine aminopeptidase, *Adv. Enzymol.* 68 (1994) 153–213.
- [64] D. Ben-Meir, A. Spungin, R. Ashkenazi, S. Blumberg, Specificity of *Streptomyces griseus* aminopeptidase and modulation of activity by divalent metal ion binding and substitution, *Eur. J. Biochem.* 212 (1993) 107–112.
- [65] C. Stamper, B. Bennett, T. Edwards, R.C. Holz, D. Ringe, G. Petsko, Inhibition of the aminopeptidase from *Aeromonas proteolytica* by L-leucinephosphonic acid. Spectroscopic and crystallographic characterization of the transition state of peptide hydrolysis, *Biochemistry* 40 (2001) 7035–7046.
- [66] P.J. O'Brien, D. Herschlag, Catalytic promiscuity and the evolution of new enzymatic activities, *Chem. Biol.* 6 (1999) R91–R105.
- [67] S.D. Copley, Enzymes with extra talents: moonlighting functions and catalytic promiscuity, *Curr. Opin. Chem. Biol.* 7 (2003) 265–272.
- [68] A. Yarnell, The power of promiscuity, *C&EN News* 8 (2003) 33–35, December.
- [69] U.T. Bornscheuer, R.J. Kazlauskas, Catalytic promiscuity in biocatalysis: using old enzymes to form new bonds and follow new pathways, *Angew. Chem. Int. Ed.* 43 (2004) 6032–6040.
- [70] R.J. Kazlauskas, Enhancing catalytic promiscuity for biocatalysis, *Curr. Opin. Chem. Biol.* 9 (2005) 195–201.
- [71] A. Radzicka, R. Wolfenden, A proficient enzyme, *Science* 26 (1995) 90–93.
- [72] D.B. Northrop, Rethinking fundamentals of enzyme action, *Adv. Enzymol. Relat. Areas Mol. Biol.* 73 (1999) 25–55.
- [73] P.F. Mugford, V.P. Magloire, R.J. Kazlauskas, Unexpected subtilisin-catalyzed hydrolysis of a sulfonamide bond in preference to a carboxamide bond in *N*-acyl sulfonamides, *J. Am. Chem. Soc.* 127 (2005) 6536–6537.
- [74] B.K. Takasaki, La(III)-hydrogen peroxide cooperativity in phosphate diester cleavage: A mechanistic study, *J. Chin, J. Am. Chem. Soc.* 117 (1995) 8582–8585.
- [75] J. Chin, M. Banaszczuk, V. Jubian, X. Zou, Cobalt(III) complex-promoted hydrolysis of phosphate diesters: comparison in reactivity of rigid *cis*-diaquo(tetraaza)cobalt(III) complexes, *J. Am. Chem. Soc.* 111 (1989) 186–190.
- [76] A.J. Kirby, M. Younas, Reactivity of phosphate esters—diester hydrolysis, *J. Chem. Soc. B* (1970) 510–513.
- [77] E.L. Hegg, J.N. Burstyn, Toward the development of metal-based synthetic nucleases and peptidases: a rationale and progress report in applying the principles of coordination chemistry, *Coord. Chem. Rev.* 173 (1998) 133–165.
- [78] N.H. Williams, B. Takasaki, M. Wall, J. Chin, Structure and nuclease activity of simple dinuclear metal complexes: Quantitative dissection of the role of metal ions, *Accounts Chem. Res.* 32 (1999) 485–493.
- [79] A. Blasko, T.C. Bruice, Recent studies of nucleophilic, general-acid, and metal ion catalysis of phosphate diester hydrolysis, *Accounts Chem. Res.* 32 (1999) 475–484.
- [80] E. Kimura, Model studies for molecular recognition of carbonic anhydrase and carboxypeptidase, *Accounts Chem. Res.* 34 (2001) 171–179.
- [81] T. Koike, E. Kimura, Roles of zinc(II) ion in phosphatases. A model study with zinc(II)-macrocyclic polyamine complexes, *J. Am. Chem. Soc.* 113 (1991) 8935–8941.
- [82] E. Kimura, H. Hashimoto, T. Koike, Hydrolysis of lipophilic esters catalyzed by a Zinc(II) complex of a long alkyl-pendant macrocyclic tetramine in Micellar solution, *J. Am. Chem. Soc.* 118 (1996) 10963–10970.
- [83] C. Bazzicalupi, A. Bencini, A. Bianchi, V. Fusi, C. Giorgi, P. Paoletti, B. Valtancoli, D. Zanchi, Carboxy and phosphate esters cleavage with mono- and di-nuclear zinc(II) macrocyclic complexes in aqueous solution, crystal structure of $[Zn_2L(\mu-PP)_2(MeOH)_2](ClO_4)_2$ (L1 = [30]aneN6O4, PP = diphenyl phosphate), *Inorg. Chem.* 36 (1997) 2784–2790.
- [84] W.H. Hapman, R. Breslow, Selective hydrolysis of phosphate esters, nitrophenyl phosphates and UpU, by dimeric zinc complexes depends on the spacer length, *J. Am. Chem. Soc.* 117 (1995) 5462–5469.
- [85] A. Bencini, E. Berni, A. Bianchi, V. Fedi, C. Giorgi, P. Paoletti, B. Valtancoli, Carboxy and diphosphate ester hydrolysis promoted by dinuclear zinc(II) macrocyclic complexes. Role of Zn(II)-bound hydroxide as the nucleophilic function, *Inorg. Chem.* 38 (1999) 6323–6325.
- [86] D. Herschlag, P.J. O'Brien, Functional interrelationships in the alkaline phosphatase superfamily: phosphodiesterase activity of *Escherichia coli* alkaline phosphatase, *Biochemistry* 40 (2001) 5691–5699.
- [87] S.B. Dotson, C.E. Smith, C.S. Ling, G.F. Barry, G.M. Kishore, Identification, characterization and cloning of a phosphonate monoester hydrolase from *Burkholderia caryophylli* PG2982, *J. Biol. Chem.* 271 (1996) 25754–25761.
- [88] H. Shim, S.-B. Hong, F.M. Raushel, Hydrolysis of phosphodiester through transformation of the bacterial phosphotriesterase, *J. Biol. Chem.* 273 (1998) 17445–17450.
- [89] S.J. Kelly, D.E. Dardinger, L.G. Butler, Hydrolysis of phosphonate esters catalyzed by 5'-nucleotide phosphodiesterase, *Biochemistry* 14 (1975) 4983–4988.
- [90] S.J. Kelly, L.G. Burtler, Enzymic hydrolysis of phosphonate esters, *Biochem. Biophys. Res. Commun.* 66 (1975) 316–321.
- [91] A. Vogel, O. Schilling, M. Niecke, J. Bettmer, W. Meyer-Klaucke, ElaC encodes a novel binuclear zinc phosphodiesterase, *J. Biol. Chem.* 277 (2002) 29078–29085.
- [92] W.W. Cleland, A.C. Hengge, Mechanisms of phosphoryl and acyl transferase, *FASEB J.* 9 (1995) 1585–1594.
- [93] M.A. Anderson, H. Shim, F.M. Raushel, W.W. Cleland, Hydrolysis of phosphotriesters: determination of transition states in parallel reactions by heavy-atom isotope effects, *J. Am. Chem. Soc.* 123 (2001) 9246–9253.
- [94] L. Que, A.E. True, Dinuclear iron- and manganese-oxo sites in biology, *Prog. Inorg. Chem.* 38 (1990) 97–200.